Relationship Between an Abrupt Drought-Flood Transition over Mid-Low Reaches of the Yangtze River in 2011 and the Intra-seasonal Oscillation over Mid-High Latitudes of East Asia

YANG Shuangyan[1] (杨双艳), WU Bingyi[1*] (武炳义), ZHANG Renhe[1] (张人禾),

and ZHOU Shunwu[2] (周顺武)

1 *Chinese Academy of Meteorological Sciences, Beijing* 100081

2 *Key Laboratory of Meteorological Disaster of Ministry of Education, NUIST, Nanjing* 210044

(Received February 3, 2012; in final form December 22, 2012)

ABSTRACT

NCEP/NCAR daily reanalysis data and Chinese daily gridded precipitation data are used to study the relationship between an aprupt drought-flood transition over the mid-low reaches of the Yangtze River in 2011 and the intraseasonal oscillation (ISO; 30–60 days) in the mid-high latitude meridional circulation of the upper troposphere over East Asia. The abrupt transition from drought to flood occurs in early June. The first two recovered fields of the complex empirical orthogonal function show that northward-propagating westerlies from low latitudes converge with southward-propagating westerlies from high latitudes over the mid-low reaches of the Yangtze River (MLRYR) in mid–late May. The timing of this convergence corresponds to the flood period in early–mid June. The ISO index is significantly and positively correlated with rainfall over the MLRYR. During the dry phase (before the transition), the upper troposphere over the MLRYR is characterized by cyclonic flow, easterly winds, and convergence. The regional circulation is dominated by a wave train with a cyclone over east of Lake Baikal, an anticyclone over northern China, and a cyclone over the MLRYR. During the wet phase, the situation is reversed. The configuration of the wave train during the dry phase favors the southward propagation of westerly wind disturbances, while the configuration of the wave train during the wet phase favors the development and maintenance of a pumping effect and sustained ascending motions over the MLRYR.

Key words: intraseasonal oscillation, the East Asian mid-high latitude area, the mid-low reaches of the Yangtze River, drought-flood abrupt alternation

Citation: Yang Shuangyan, Wu Bingyi, Zhang Renhe, et al., 2013: Relationship between an abrupt drought-flood transition over mid-low reaches of the Yangtze River in 2011 and the intraseasonal oscillation over mid-high latitudes of East Asia. *Acta Meteor. Sinica*, **27**(2), 129–143, doi: 10.1007/s13351-013-0201-0.

1. Introduction

An atmospheric intraseasonal oscillation (ISO) is generally a low-frequency oscillation with a period of 30–60 days. Madden and Julian (1971) discovered the existence of an ISO in the tropics at the beginning of the 1970s by applying a spectral analysis to observational data from Canton Island. Madden and Julian (1972) then confirmed that the ISO (which is often referred to as the Madden-Julian oscillation, or MJO) exists throughout the global tropics. Subsequent studies have shown that such low-frequency oscillations exist not only in the tropics (Lau and Chan, 1985; Li and Wu, 1990), but also in mid-high latitudes (Anderson and Rosen, 1983; Zhang, 1987), and even over the entire globe (Li, 1991). Zhang et al. (1992) showed that the ISO results from the internal dynamics of the atmosphere and is inherent in both the tropics and mid-high latitudes. Sun et al. (2008, 2010) have recently applied current understanding of ISO to extended-

Supported by the National Natural Science Foundation of China (41221064 and 40875052), China Meteorological Administration Special Public Welfare Research Fund (GYHY200906017 and GYHY201006020), and Basic Research Fund of the Chinese Academy of Meteorological Sciences (2010Z003).

*Corresponding author: wby@cams.cma.gov.cn.

range precipitation forecasts. ISO is not a local but rather a global phenomenon, and therefore affects not only local precipitation but also monsoons (Qi et al., 2008; Sun and Ding, 2008), the El Niño-Southern Oscillation (ENSO) (Li and Zhou, 1994), tropical cyclones (Tian et al., 2010; Sun et al., 2009; Zhu and Li, 2004), and global weather and climate patterns (Zhang, 2005).

The influences of ISO on Chinese and East Asian rainfall have received increased attention in recent years. Jeong et al. (2008) found that the MJO significantly modulates the distribution of wintertime precipitation over four East Asian countries. Yuan and Yang (2010) reported a strong MJO influence on rainfall over northeastern China during winter. Zhang et al. (2011) noted that the intensity of rainfall in South China during the first rainy season changes from heavy to light when the MJO active center moves from the Indian Ocean to the western Pacific. Ding et al. (2004) reported that the northward propagation of the ISO over the South China Sea can enhance rainfall over China and East Asia during seasonal transitions. Jia and Guan (2010) defined an ISO-based intensity index for interannual variability in precipitation over the Yangtze-Huaihe River basin (YHRB). They found a significant correlation between rainfall anomalies over the YHRB and ISO energetics over the Taiwan Strait and western Pacific.

The studies mentioned above focused solely on ISO over low-latitude areas, but ISO over mid-high latitudes (MHL) may also affect East Asian rainfall. Ju et al. (2008) confirmed that zonal-propagating ISO circulations merge with meridional-propagating circulations in the subtropics. Yang and Li (2003) showed that the influences of ISO activity at 500 and 200 hPa over the YHRB, northern China, and MHL to the north of China are stronger during severe floods than during severe droughts. ISO-related meridional wind disturbances over MHL can propagate southward and converge with northward-propagating meridional wind disturbances associated with low-latitude ISO. This convergence is observed over the YHRB during years with severe flooding, but not during years with severe drought. Ju et al. (2005a, b) noted that ISOs follow a “monsoon stream” pattern during the East Asian summer monsoon. As an ISO moves northward with time, differences in its magnitude at different latitudes reflect differences in local large-scale rainfall processes. The ISO enhances rainfall over the mid-low reaches of the Yangtze River (MLRYR) during active East Asian monsoon years. Han et al. (2006) discovered that drought-flood transitions over East Asia during summer are closely correlated with westward movement of the ISO in the central and eastern Pacific with subtropical easterly winds. These transitions are also closely correlated with southwestward movement of low-frequency disturbances that pass the subtropical North Pacific during long-wave adjustment over MHL. The ISO over MHL has a clear relationship with rainfall anomalies over China and East Asia; however, the link between upper tropospheric ISO and these rainfall anomalies remains unclear.

An abrupt drought-flood transition occurred over the MLRYR in 2011. Such abrupt transitions often occur in China during boreal summer, but this event has not yet been discussed in detail. Most past studies have been based on anomalies in total precipitation during summer. Less attention has been paid to intraseasonal changes, which are as important as total summer rainfall for socioeconomic concerns such as quality of life, water resource allocation, and industrial and agricultural production. Abrupt drought-flood transitions are one type of intraseasonal rainfall variation. Wang et al. (2009) discussed the climatic characteristics of these transitions during the principal flood season over the YHRB. Wu et al. (2006) investigated the correlation between long-period abrupt transitions (both drought-to-flood and flood-to-drought) over the MLRYR during the summer and large-scale circulation anomalies. The current study focuses on an abrupt transition from drought to flood over the MLRYR during 2011. The relationship between this transition and ISO is explored by focusing on the correlation between the evolution of the ISO in the meridional circulation of the upper troposphere (200 hPa) and precipitation over the MLRYR. The characteristics of the meridional circulation during this abrupt transition provide useful insight for future attempts to forecasting precipitation over the MLRYR.

2. Data and methodology

The daily gridded precipitation is obtained from the Chinese real-time analytic system (version 1.0), which has a latitude-longitude horizontal resolution of 0.25°×0.25°. The data are obtained by performing optimal interpolation on daily precipitation from 2419 Chinese stations based on climatic background fields. The MLRYR is defined as the area 28°–32°N, 110°–122°E.

The daily gridded reanalysis data are provided by NCEP/NCAR, and have a horizontal resolution of 2.5°×2.5° (Kalnay et al., 1996). The reanalysis data include zonal wind (u), meridional wind (v), and temperature (T). The vertical vorticity (ζ_p) in spherical coordinates is calculated at the standard isobaric surfaces (1000, 925, 850, 700, 600, 500, 400, 300, 250, 200, 150, and 100 hPa). Isentropic potential vorticity (IPV) at the 325-K isentropic surface is calculated as described by Hoskins et al. (1985), i.e., vorticity is first calculated on isobaric surface and IPV is then computed via linear interpolation.

The seasonal cycle is removed from all reanalysis data. The prevalent period of the height and wind fields at 200 hPa over the MLRYR was 30–60 days in 2011. Each field is processed using a Butterworth band-pass filter (Murakami, 1979). The filtered u, v, ζ_p, and IPV are denoted throughout this paper by u', v', ζ'_p, and IPV$'$, respectively.

The abrupt change in rainfall is tested using the Mann-Kendall method (Wei, 2007) and evaluated using complex empirical orthogonal function analysis (CEOF) (Barnett, 1983). The circulation fields are reconstructed using the complex eigenvectors and time coefficients from the first two CEOF modes, as in Wu et al. (1994).

3. Basic features of the abrupt drought-flood transition

More than 90% of the MLRYR region was affected by drought between early April and late May of 2011. The water levels in some channels of the Yangtze River fell below 15 m, and millions of people were confronted with drinking water shortages in Hubei, Hunan, Jiangxi, Anhui, and Jiangsu provinces. This situation changed abruptly on 3 June 2011, with the provinces of Jiangxi, Hunan, Guizhou, and Zhejiang receiving heavy rain and storms after 3 June. Figure 1 shows the distribution of mean precipitation in China during the drought period (from 1 May to 2 June; Fig. 1a) and the flood period (from 3 June to 1 July; Fig. 1b). The daily mean rainfall was less than 10 mm day^{-1} over the MLRYR (the rectangular area) for one month prior to 3 June. The largest rainfall during this period was located to the south of the Yangtze River, with a peak rain rate of 20 mm day^{-1} (Fig. 1a). By contrast, the largest rainfall after 3 June was centered over the MLRYR, with peak rain rates of more than 30 mm day^{-1}. The mean rainfall

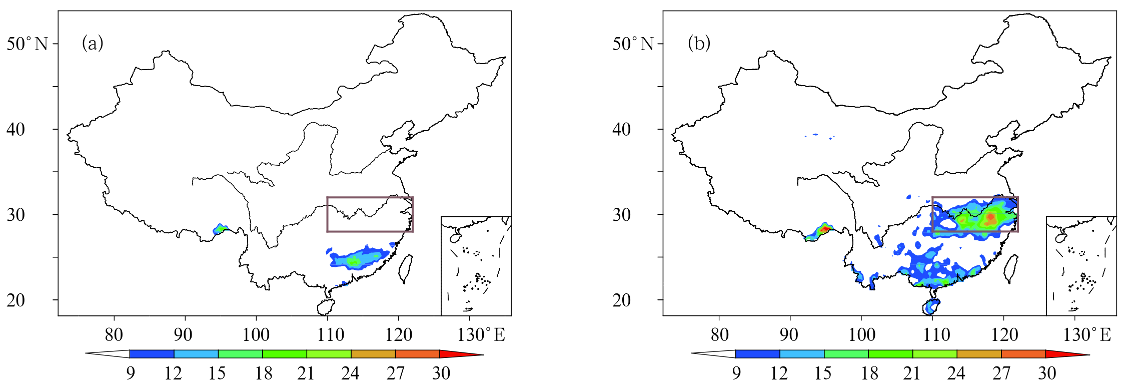

Fig. 1. Distributions of precipitation (mm day^{-1}) in China during (a) the drought period (1 May–2 June) and (b) the flood period (3 June–1 July) of 2011. The rectangular indicates the mid-low reaches of the Yangtze River.

in other regions was less than 9 mm day^{-1}, except for some small areas of South China and Tibet. This shows that the daily mean rainfall in the MLRYR changed abruptly from low to high on 3 June. In the following discussion, the regional average daily mean precipitation refers to daily mean rainfall in the MLRYR.

The characteristics of the drought-flood transition are investigated using the time series of the regional rainfall anomaly from 1 March to 1 July 2011 (Fig. 2a). The rain anomaly was predominantly negative before 3 June, with positive anomalies occurring only intermittently. The anomaly then changed to predominantly positive on 3 June and remained predominantly positive for 2–3 weeks. This result confirms that mean rainfall in the MLRYR transitioned abruptly from below average to above average in early June. The exact timing of this shift is identified using the Mann-Kendall method (Fig. 2b). UF and UB are two statistical variables that are functions of mathematical expectation and variance. UF and UB are derived with estimation U based on forward and backward orders of time series of daily rainfall, respectively. The increase in rainfall in early June is evident in the UF testing curve, and passed the 5% significance level on 16 June. The intersection of the UF line and UB line indicates that the shift occurred on 1 June. These results show from a statistical perspective that this abrupt transition from drought to flood exists, and the shift occurred in early June. This transition is several weeks earlier than the typical date of drought-flood transitions obtained by Wu et al. (2006) who indicated that the transition date is late June.

4. Correlations between precipitation and the ISO circulation

4.1 The East Asian mid-high latitude ISO before and after the shift

The basic characteristics of the ISO circulation are analyzed in this section. Slingo et al. (1996, 1999) proved that ISO activity can be represented by u'; the following analysis therefore focuses on u' at 200 hPa. The spatio-temporal distribution of rainfall from 1 March to 1 July is analyzed using CEOF. The two leading modes of the CEOF, i.e., CEOF1 and CEOF2, contribute 55.89% and 24.88% of the variance, respectively. The error ranges of the eigenvalues show that CEOF1 and CEOF2 are statistically independent from higher-order modes (North et al., 1982). The primary features during the shift period are reconstructed as in Wu et al. (1994). Figure 3a shows a latitude-time cross-section of this reconstruction at 120°E. The sum of the first two reconstruction fields is adequate for examining the primary features of u' because the first two CEOF modes contribute to such a high proportion (80.77%) of the total variance.

A westerly wind disturbance propagated northward from low to high latitudes in mid–late April. This propagation continued until the westerly wind disturbance approached 50°N on 16 May. After that date, the disturbance propagated southward from

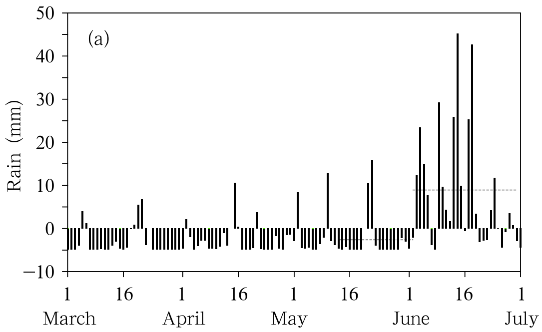

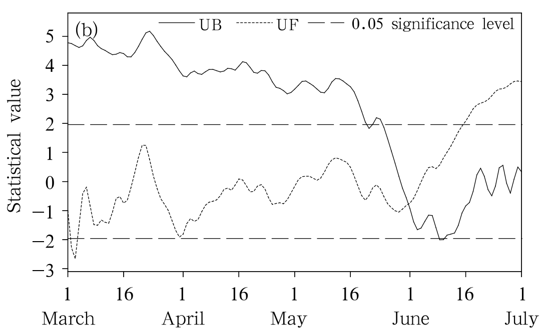

Fig. 2. (a) Daily rainfall anomaly (mm) in the MLRYR. The two horizontal dotted lines denote the mean anomalies from 13 May to 2 June and from 3 June to 1 July 2011. (b) Mann-Kendall test curves for the time series of daily rainfall anomaly. The dashed line indicates the critical value for 5% significance from 1 March to 1 July 2011.

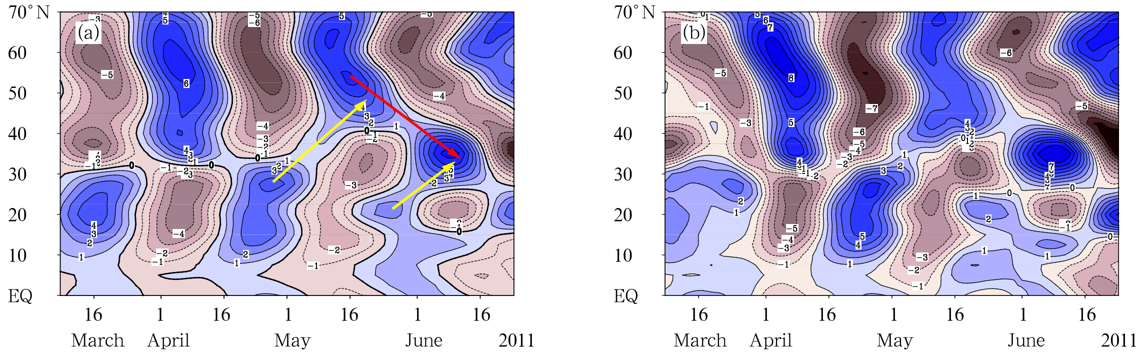

Fig. 3. Latitude-time cross-sections along 120°E of (a) u' reconstructed from CEOF1 and CEOF2 and (b) u' from the raw data. Blue and gray shadings denote westerly and easterly wind disturbances, respectively. The contour interval is 1 m s^{-1} and the arrows indicate the direction of propagation.

50°N toward lower latitudes. At the same time, another northward-propagating westerly wind disturbance moved from approximately 20°N to mid latitudes. These two westerly wind disturbances converged over the MLRYR in mid June, creating a strong local westerly wind anomaly with a maximum value of approximately 8 m s^{-1}. An easterly wind anomaly developed over the area to the south of the MLRYR at about the same time (Fig. 3b). The upper tropospheric circulation over the MLRYR was therefore dominated by an anticyclonic anomaly in early–mid June, which favored local divergence. The zonal wind anomaly over the MLRYR in mid–late May was easterly, while that in the area to the south of the MLRYR was westerly (Fig. 3b). The anomalous circulation in the upper troposphere over the MLRYR in mid–late May was therefore opposite to that in early–mid June, with a cyclonic anomaly that favored local convergence.

To summarize, the upper tropospheric circulation was characterized by an easterly wind disturbance and anomalous convergence over the MLRYR during the drought period. By contrast, the upper tropospheric circulation was characterized by a westerly wind disturbance and anomalous divergence during the flood period. Convergence in the upper troposphere promotes subsidence, while divergence promotes ascent. These characteristic vertical motions aided in the development of the drought and flood events, with local subsidence acting to suppress precipitation and local ascent acting to enhance it.

The analysis in Section 3 indicates that the abrupt transition from drought to flood occurred on 1 June. The zonal wind anomalies in the area immediately north and south of 25°N switched on approximately the same day. An easterly wind anomaly north of 25°N switched to westerly, while a westerly wind anomaly south of 25°N switched to easterly. The rainfall anomaly was evidently different between the drought and flood periods (Fig. 2a). The differences in the ISO circulation of the upper troposphere at MHL between the two periods are evaluated using separate composites of u', v', and ζ'_p for the two periods (Fig. 4). The upper tropospheric circulation over the MLRYR was characterized by cyclonic vorticity and an easterly zonal wind anomaly during the drought period, but by anticyclonic vorticity and a westerly zonal wind anomaly during the flood period. The (unfiltered) 5880-gpm isoline associated with the western Pacific subtropical high extended more westward in early–mid June than in mid–late May. This westward extension enhanced water vapor transport into the MLRYR region from lower latitudes along the southern flank of the subtropical high. Cooperation between the upper- and lower-level circulation systems during the different periods therefore led to the abrupt drought-flood transition. Figure 4 shows a positive-negative-positive vorticity pattern in mid–late May, which switches to a negative-positive-negative pattern in mid–early June. The three centers of this

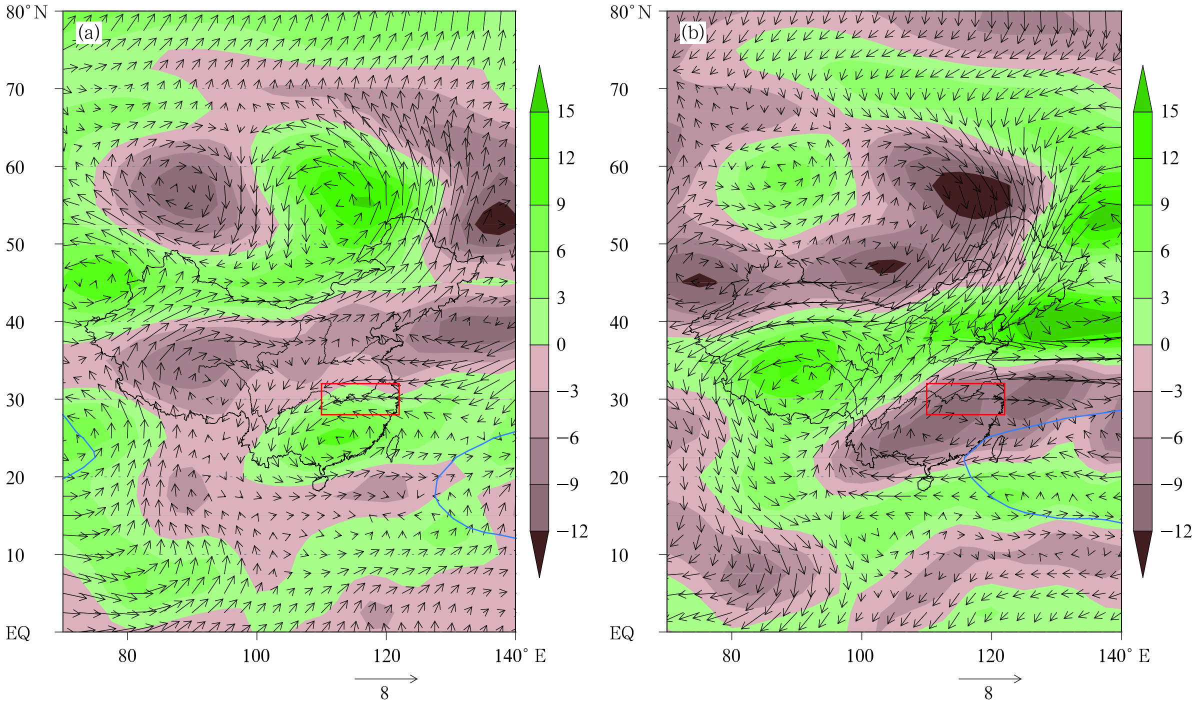

Fig. 4. Reconstructions of u', v' (vectors; m s^{-1}), and ζ'_p (shaded; 10^{-6} s^{-1}) at 200 hPa during (a) the period of low rainfall from 15 to 31 May 2011 and (b) the period of enhanced rainfall from 3 to 19 June 2011. The blue line indicates the unfiltered 5880-gpm isoline, and green and gray shadings denote positive and negative vorticity anomalies, respectively.

pattern were located over the east of Lake Baikal (positive then negative), northern China (negative then positive), and the MLRYR (positive then negative). The remainder of this paper focuses on the link between variations in this circulation pattern during the drought and flood periods and the abrupt transition between them.

4.2 Definition of the ISO index

Changes in ζ'_p, which reflect circulation variability, appear to correspond well with changes in rainfall during the drought-flood transition. Figure 5 shows the spatial distribution of the correlation coefficient between rainfall over the MLRYR and 200-hPa ζ'_p between 1 March and 1 July 2011. These correlation coefficients follow a negative-positive-negative pattern from the east of Lake Baikal in the north to the MLRYR in the south. Three key areas (A, B, and C) are selected to represent this negative-positive-negative pattern. The longitudinal scope of each key area is 110°–120°E, and their latitudinal scopes are 50°–60°N, 36°–43°N, and 22°–32°N, respectively. The average correlation coefficients of A ($R_{\rm A}$), B ($R_{\rm B}$), and C ($R_{\rm C}$) are –0.3085, 0.3276, and –0.2500, respectively. The weighted ISO index ($I_{\rm ISO}$) is defined by the following equation:

$$I_{\rm ISO}=\frac{|R_{\rm B}|\zeta'_{\rm B}}{|R_{\rm A}|+|R_{\rm B}|+|R_{\rm C}|}-\frac{|R_{\rm A}|\zeta'_{\rm A}}{|R_{\rm A}|+|R_{\rm B}|+|R_{\rm C}|}-\frac{|R_{\rm C}|\zeta'_{\rm C}}{|R_{\rm A}|+|R_{\rm B}|+|R_{\rm C}|}, \quad (1)$$

where $\zeta'_{\rm A}$, $\zeta'_{\rm B}$, and $\zeta'_{\rm C}$ (in 10^{-6} s^{-1}) represent the average vorticity anomaly in each key area and $\frac{|R_{\rm A}|}{|R_{\rm A}|+|R_{\rm B}|+|R_{\rm C}|}$, $\frac{|R_{\rm B}|}{|R_{\rm A}|+|R_{\rm B}|+|R_{\rm C}|}$, and $\frac{|R_{\rm C}|}{|R_{\rm A}|+|R_{\rm B}|+|R_{\rm C}|}$ are weighting coefficients. The sign of the coefficient $R_{\rm B}$ is opposite to those of $R_{\rm A}$ and $R_{\rm C}$ (Fig. 5); therefore, the weighting coefficient for $R_{\rm B}$ is opposite in sign to those for $R_{\rm A}$ and $R_{\rm C}$. $I_{\rm ISO}$ is the weighted sum of the ISO vorticity anomaly in the three key areas. Changes in vorticity reflect changes in the circulation, so Eq. (1) expresses the

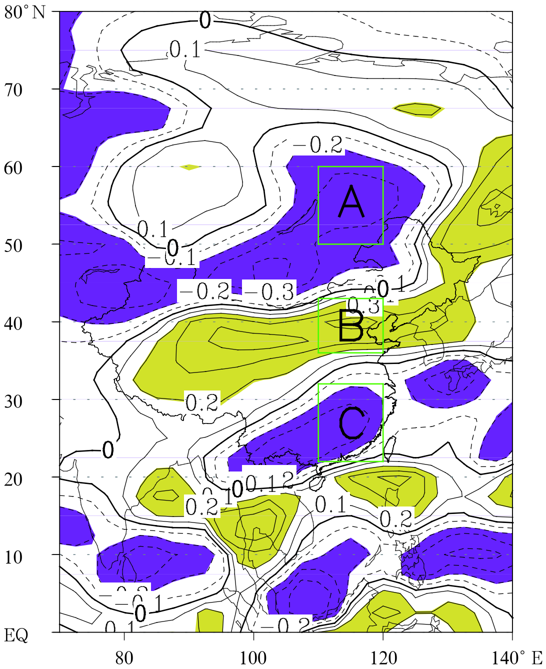

Fig. 5. Spatial distribution of the correlation coefficient between rainfall over mid-low reaches of the Yangtze River and 200-hPa ζ'_p between 1 March and 1 July 2011. Shadings indicate statistical significance at the 5% level, with dark and light shadings indicating negative and positive correlations, respectively. The key regions A, B, and C are marked as rectangular areas.

state of the ISO circulation over the MHL of Eurasia. This state evidently affects the abrupt drought-flood transition in the MLRYR.

Figure 6a shows the time series of $I_{\rm ISO}$ and rainfall over the MLRYR. The correlation coefficient between the two series is 0.4387. The structure of the ISO time series over this time period is wavenumber 3. The largest amplitude cycle in this wavenumber-3 pattern occurred during mid May and late June, with the drought and flood periods corresponding to the negative and positive phases of the cycle, respectively. The minimum $I_{\rm ISO}$ during this cycle (approximately -9.3×10^{-6} s^{-1}) occurred on 21 May and the maximum $I_{\rm ISO}$ (approximately 13.8×10^{-6} s^{-1}) occurred on 15 June. The correlation between the time series of $I_{\rm ISO}$ and the ISO rainfall anomaly is considerably higher, with a correlation coefficient of 0.8717 (Fig. 6b). The amplitude and phase of the $I_{\rm ISO}$ series correspond almost exactly to the amplitude and phase of the ISO rainfall series over this period. The ISO rainfall anomaly explains approximately 36.3% of the total variance in rainfall. $I_{\rm ISO}$ as defined above is well correlated with MLRYR precipitation and successfully reflects the characteristics of the abrupt drought-flood transition. The most intense wave cycle of the $I_{\rm ISO}$ is divided into eight phases according to the method described by Mao and Wu (2005). Phases 1 and 5 are transitional phases, with Phase 1 representing a transition from positive to negative and Phase 5 representing a transition from negative to positive. Phases 3 and 7 represent the trough and crest of the wave cycle, respectively.

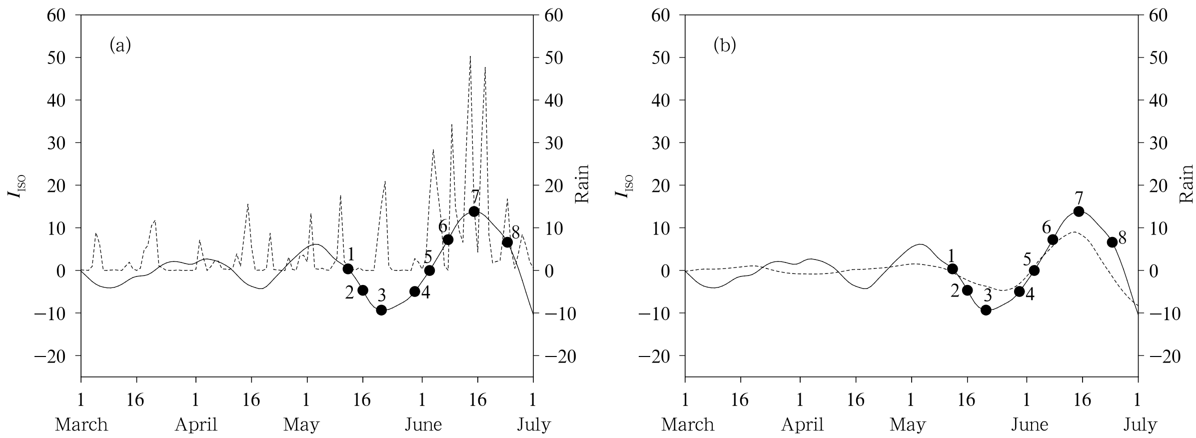

Fig. 6. (a) Observed precipitation (dashed line; mm) and (b) ISO precipitation (dashed line; mm) over the MLRYR from 1 March to 1 July 2011. The ISO index time series (solid line; 10^{-6} s^{-1}) is shown in both panels, with the eight phases marked by the numbers 1 to 8.

Phases 2, 4, 6, and 8 represent the times when the amplitude reaches half-minimum or half-maximum. The dates of each phase are provided in Table 1 (the labels correspond to the numbers plotted in Fig. 6). Phases 1 to 4 correspond to the drought period and together make up the "dry phase", while phases 5 to 8 correspond to flood period and together make up the "wet phase". The evolution of the ISO circulation from the drought period to the flood period is explored in the next section.

Table 1. Dates corresponding to each phase of the ISO index during the drought and flood periods

Category	Phase	Date	Phase	Date	Phase	Date	Phase	Date
Dry phase	1	12 May 2011	2	16 May 2011	3	21 May 2011	4	30 May 2011
Wet phase	5	3 June 2011	6	8 June 2011	7	15 June 2011	8	24 June 2011

4.3 Evolution of the ISO circulation

The results presented above show a clear connection between ISO-related circulation variability and the abrupt transition from drought to flood in the MLRYR. We now examine the evolution of ζ_p', u', and v' with respect to the phases of the ISO. The value of each variable is defined for each phase by taking a 3-day mean centered on the date of the phase as listed in Table 1.

Figure 7 shows latitude-height cross-sections of ζ_p' in each phase, averaged between 110° and 122°E. The pattern during the dry phase was opposite to the pattern during the wet phase. During the dry phase, ζ_p' was positive in the upper troposphere and negative in the mid-lower troposphere over the MLRYR (bounded by the two yellow dotted lines). During the wet phase, the opposite was true. The pattern of ζ_p' during the dry phase indicates an ISO-related upper-level cyclone and lower-level anticyclone, while the pattern of ζ_p' during the wet phase indicates an upper-level anticyclone and a lower-level cyclone. The ISO-related circulation during the dry phase contained anomalous convergence in the upper layer and divergence in the lower layer, which favored descent over the MLRYR. By contrast, the ISO-related circulation during the wet phase contained divergence in the upper layer and convergence in the lower layer, which favored a vertical pumping effect over the MLRYR. This pumping effect, which was caused by the upper tropospheric anticyclone, led to sustained ascending motions over the MLRYR during the wet phase.

The sign of ζ_p' in the upper troposphere over the MLRYR was the same as that over the north of Lake Baikal (bounded by the two red dotted lines) and was opposite to that over northern China (bounded by the two blue dotted lines). The distribution of ζ_p' during the dry phase favored the westward propagation of zonal wind anomalies. Chen et al. (2005) concluded that the southward propagation of ISO signals from MHL is primarily caused by horizontal advection of westerly momentum and temperature. The southern flank of westerly u' in the upper troposphere was located near 35°N during the dry phases (Figs. 8a–8d), then shifted southward to approximately 25°N during the wet phases (Figs. 8e–8h). This shift is consistent with the southward propagation of westerly u' shown in Fig. 3. Chen et al. (2005) reported that the meridional circulation in the lower-mid troposphere can shift the ISO anticyclone in MHL southward, allowing the anticyclone to interact with low-latitude weather systems. The circulation pattern during the dry phase favored the southward propagation of westerly u'. The following paragraph provides a more detailed phase-by-phase analysis of the primary features of the ISO circulation.

During Phase 1, ζ_p' was negative in the upper troposphere over most of the MHL of Eurasia (Fig. 7a). The center of this negative ζ_p' was located between 30° and 40°N. The anticyclonic anomaly at MHL resulted in a negative u' (an easterly wind anomaly) at 200 hPa to the south of ∼35°N and a positive u' (a westerly wind anomaly) to the north (Fig. 8a). The circulation in the upper troposphere over the MLRYR was therefore anticyclonic, with an easterly wind anomaly. During Phase 2, ζ_p' was positive and the circulation was cyclonic in the upper troposphere over east of Lake Baikal (Fig. 7b). The value of ζ_p' transitioned from negative to positive over the MLRYR, but was still negative (with an anticyclonic circulation) over northern China. Accordingly, the zonal wind anomaly over the MLRYR was easterly (Fig. 8b). During Phase 3, ζ_p' was positive in the upper troposphere over the MLRYR (with a maximum value of more than 10×10^{-6} s^{-1}) and the zonal wind anomaly was still easterly (Fig. 7c), but the zonal wind anomaly over the area to the north of the MLRYR was gradually becoming westerly (Fig. 8c). The positive ζ_p' to the east of Lake Baikal increased from that observed during Phase 2 (Fig. 7c), leading to an easterly wind anomaly north

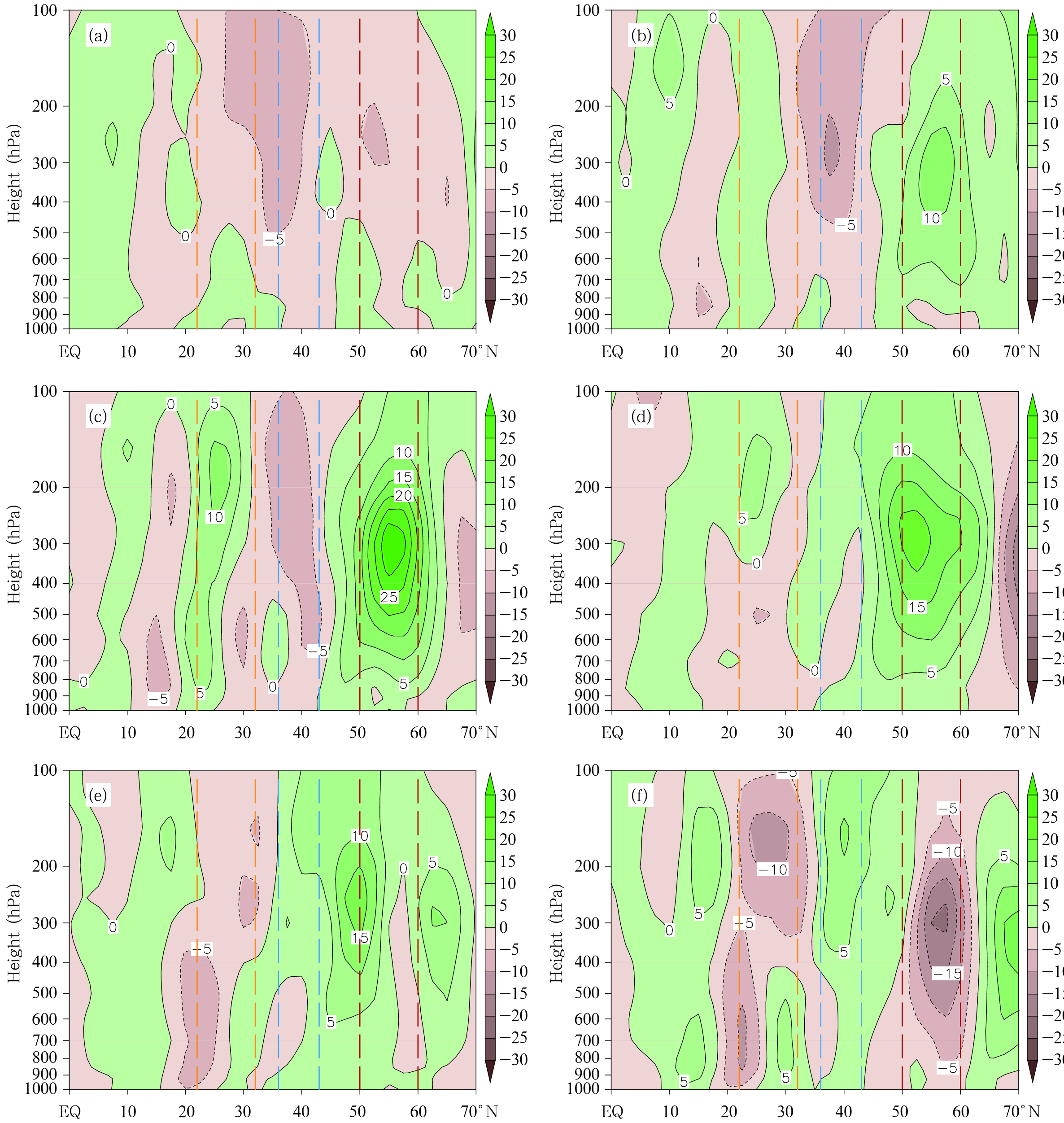

Fig. 7. Phase-by-phase evolution of latitude-height sections of ζ_p' (10^{-6} s^{-1}) averaged between 110° and 122°E. (a)–(h) denote phases 1–8 respectively. Green and gray shadings indicate positive and negative values of ζ_p', respectively. The yellow, blue, and red dashed vertical lines denote the latitude ranges of areas A, B, and C, respectively (see Fig. 6).

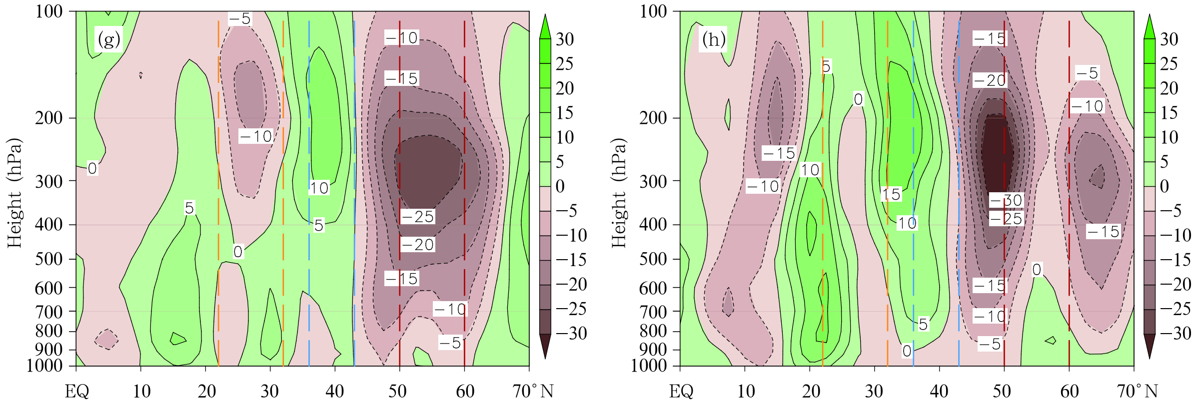

Fig. 7. (Continued.)

of 55°N (Fig. 8c). Phase 3 was the most intense dry phase, and contained the strongest positive value of upper tropospheric ζ_p' over the MLRYR. By contrast, Phase 4 was a decaying phase. The maximum ζ_p' in the upper troposphere over the MLRYR (5×10^{-6} s^{-1}) was half that observed in Phase 3. Moreover, ζ_p' was already weakly positive over northern China (Fig. 7d). This change caused the high-latitude westerly wind anomaly to propagate southward and weakened the easterly wind anomaly in the upper troposphere over the MLRYR (Fig. 8d). Phases 5 and 6 were transitional phases between the dry phase and the wet phase. Upper tropospheric ζ_p' gradually became negative over both the MLRYR and the east of Lake Baikal, and positive over northern China (Figs. 7e–7f). The zonal wind anomaly in the upper troposphere over the MLRYR became westerly, while that over the south of the MLRYR became easterly (Figs. 8e–8f). Phase 7, which contained the strongest negative value of upper tropospheric ζ_p' over the MLRYR (more than 10×10^{-6} s^{-1}), was the most intense wet phase. The values of ζ_p' over the area east of Lake Baikal were also strongly negative, while those near northern China were positive (Fig. 7g). The negative-positive-negative pattern in upper tropospheric ζ_p' was accompanied by a westerly-easterly-westerly pattern in u' from high latitudes to the MLRYR, with easterly anomalies south of the MLRYR (Fig. 8g). All of the dominant patterns observed during Phase 7 are opposite to those observed during Phase 3. Phase 8 represented the decay of the wet phase. The values of ζ_p' in the upper troposphere over the MLRYR, over northern China, and over the region east of Lake Baikal were all weaker during Phase 8 than during Phase 7 (Fig. 7h). The westerly wind anomaly in the upper troposphere over the MLRYR was also substantially weakened (Fig. 8h).

The patterns of both ζ_p' and u' over the MHL of East Asia were distinctly different between the dry and wet phases. During the driest phase (Phase 3), the circulation in the upper troposphere over the MLRYR was cyclonic, with convergence and an easterly wind anomaly. These conditions do not favor precipitation. During the wettest phase (Phase 7), the circulation was anticyclonic, with divergence and a westerly wind anomaly. These conditions do favor the development of rainfall. The sign of ζ_p' over the east of Lake Baikal was also the same as that over the MLRYR during both the driest and wettest phases. The ISO-related circulation anomaly over East Asia contained a cyclonic-anticyclonic-cyclonic wave train from high latitudes (near Lake Baikal) to low latitudes (the MLRYR) during the driest phase, and an anticyclonic-cyclonic-anticyclonic wave train during the wettest phase.

5. Conclusions and discussion

NCEP/NCAR daily reanalysis data and Chinese daily gridded precipitation data have been used to an-

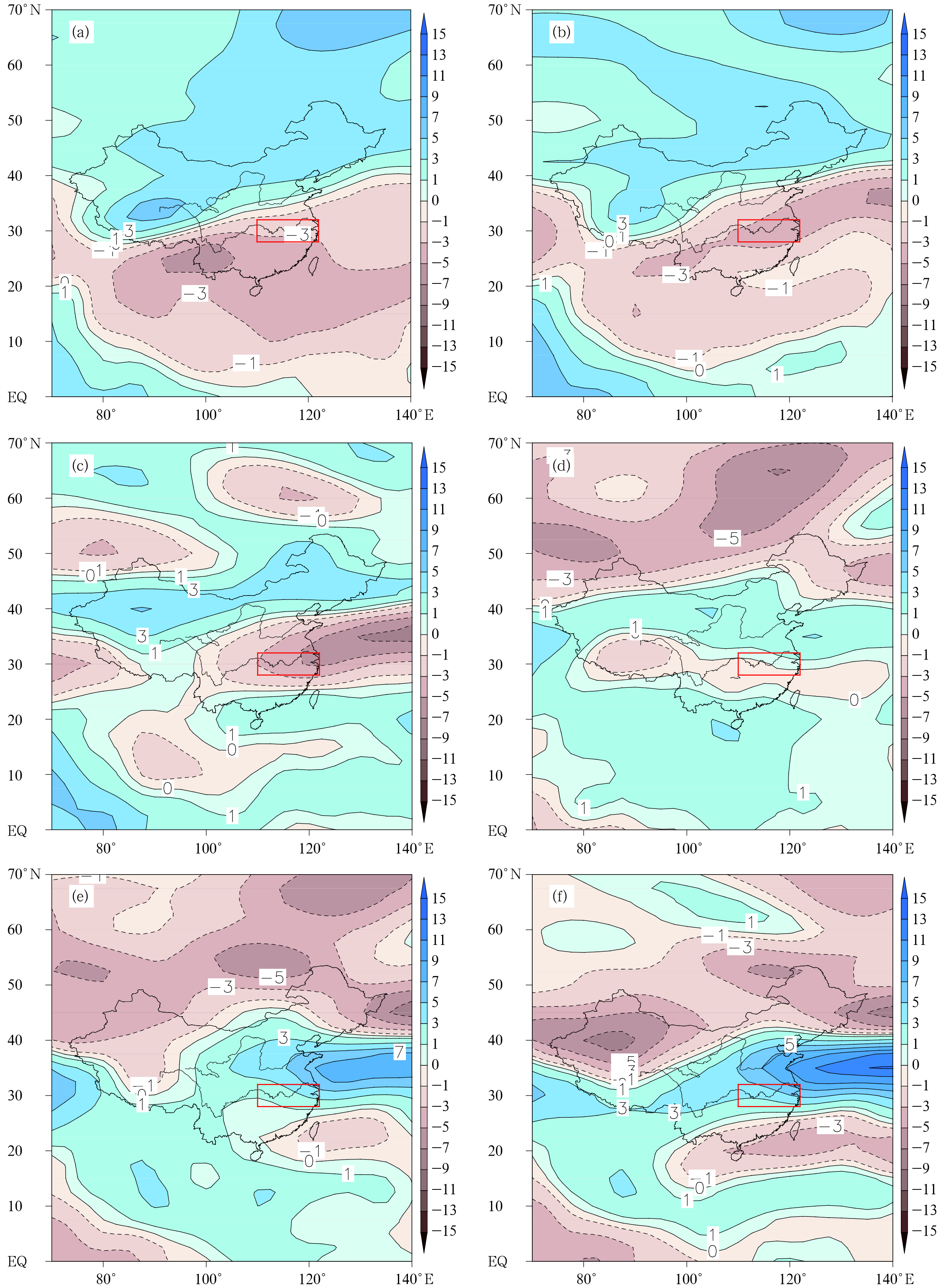

Fig. 8. Phase-by-phase evolution of the distribution of u' (m s^{-1}) at 200 hPa. (a)–(h) denote phases 1–8 respectively. Gray and blue shadings indicate the easterly and westerly wind anomalies, respectively.

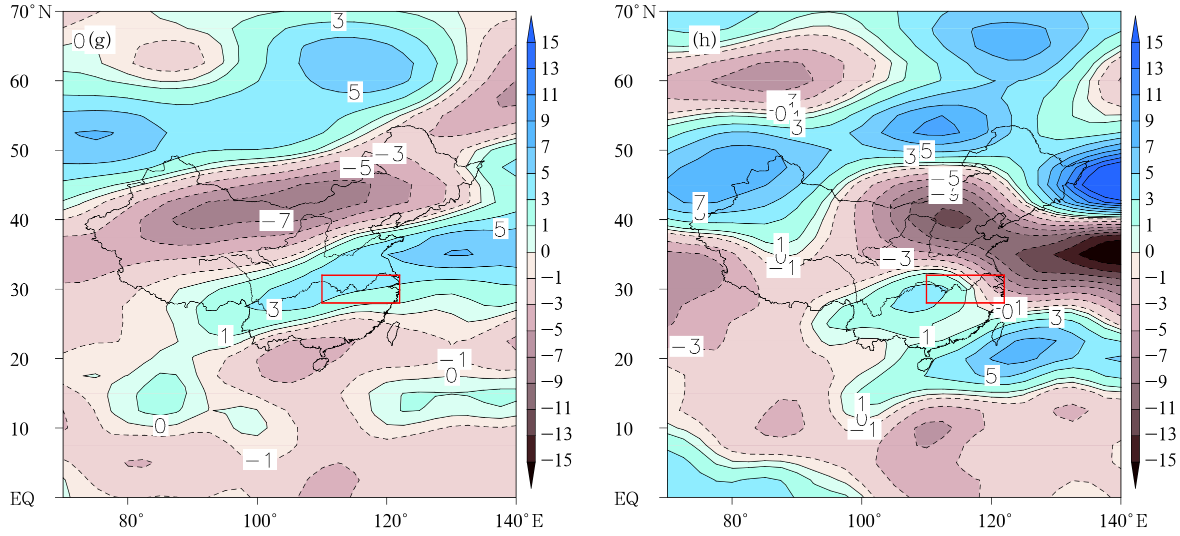

Fig. 8. (Continued.)

alyze the characteristics of the abrupt drought-flood transition over the MLRYR in May and June 2011 and its relationship with the meridional structure of the ISO circulation at mid-high latitudes over East Asia. The principal findings of the current study are as follows.

(1) The abrupt drought-flood transition over the MLRYR occurred in early June 2011. A northward-propagating 200-hPa westerly wind anomaly from low latitudes and a southward-propagating 200-hPa westerly wind anomaly from high latitudes converged in the upper troposphere over the MLRYR at the beginning of June. The upper troposphere over the MLRYR was characterized by convergence and an easterly zonal wind anomaly during the drought period. By contrast, it was characterized by divergence and a westerly wind anomaly during the flood period.

(2) The distribution of ζ'_p during the drought-flood period has been used to define an ISO index. This index is related to the MHL circulation over East Asia and is positively correlated with rainfall over the MLRYR. During the dry phase (phases 1 to 4; see Table 1 and discussion in the text), the ISO-related circulation anomaly over the MLRYR was cyclonic in the upper layer and anticyclonic in the lower layer. This circulation led to convergence in the upper layer and divergence in the lower layer, which favored descending vertical motion. The situation was reversed during the wet phase (phases 5 to 8), creating a pumping effect and sustained ascending motion over the MLRYR. The meridional cyclonic-anticyclonic-cyclonic wave train during the dry phase had a significant influence on the southward propagation of the upper tropospheric westerly wind anomaly during the drought period. The anticyclonic-cyclonic-anticyclonic wave train during the wet phase acted to maintain the pumping effect and sustained ascending motion over the MLRYR. Upper tropospheric zonal wind anomalies over the MLRYR were easterly during the drought period and westerly during the flood period.

This study has focused on the association between rainfall and the meridional circulation at MHL over East Asia, but this type of rainfall event is also affected by several other factors. These factors include the position of the western Pacific subtropical high (Wu et al., 2006; Gong et al., 2004) and ISO-related variations in the zonal circulation at high latitudes (Yang, 2001), among others. Gong et al. (2004) found that rainfall over the YHRB is centered on the northern edge of the subtropical high (at the 5880-gpm line), where high-latitude air meets midlatitude air. From the perspective of synoptic meteorology, this interaction is a convergence of cold and warm air masses. Yang (2001) studied the relationship between the interannual variability of drought-flood transitions over

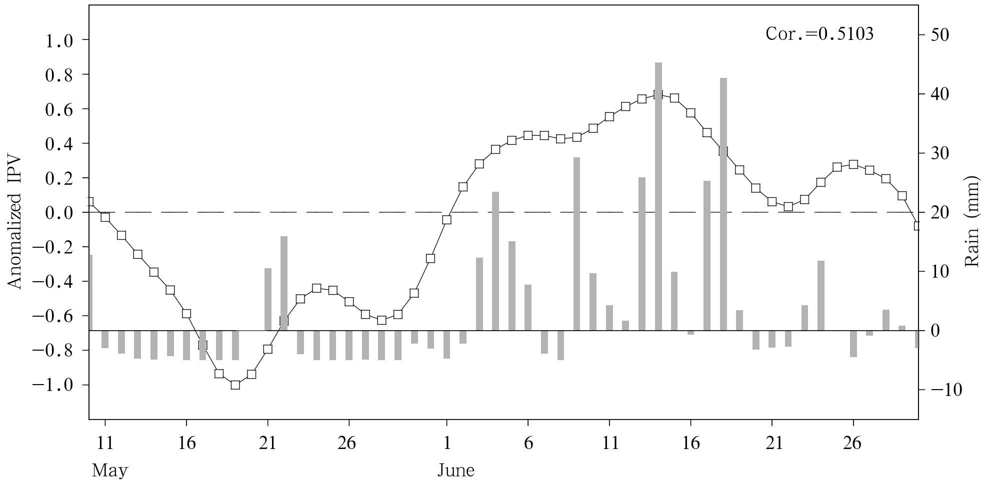

Fig. 9. Time series of IPV′ at 325 K (curve) and precipitation anomaly over the MLRYR (columns) from 10 May to 30 June 2011.

the MLRYR and ISO-related circulation variability over Eurasia during the summer season. They found wave trains propagating at MHL over Eurasia in ISO geopotential height anomalies at 500 hPa, and reported that the intensity of the wave trains was closely correlated with the frequency of flood periods. Figure 9 shows that this abrupt drought-flood transition is also closely associated with cold air supplied by the ISO circulation. Although changes in isentropic potential vorticity (IPV) are often used to represent transport of cold air (Ding and Ma, 2008; Li et al., 2010), Zhao and Ding (2009) showed that this transport is best represented by low-frequency IPV. Here, air masses near the MLRYR are represented using IPV at 325 K (Shou, 2010) averaged over the region 25°–32°N, 110°–122.5°E. The standardized IPV′ and rainfall anomaly time series are positively correlated with a correlation coefficient of 0.5103. This result indicates that the abrupt drought-flood transition over the MLRYR in 2011 was closely related to low-frequency atmospheric transport activity.

The low-frequency oscillations in the rainfall are primarily expressed in the peak value of precipitation. The negative values result from filtering. This study has focused on the correlation between low-frequency variability in the circulation and the original rainfall field; the local rainfall is therefore not a principal concern. The abrupt drought-flood transition can be discussed in terms of low-frequency variability because the original rainfall field contains a low-frequency oscillation throughout the transitional stage. This study has only analyzed the low-frequency evolution of the circulation during the period of the abrupt drought-flood transition. Additional research should examine the features and causes of this circulation variability more thoroughly.

Acknowledgments. We thank NOAA for providing the reanalysis data and the China Meteorological Administration for providing the daily gridded precipitation data. We particularly thank the anonymous reviewers for their valuable comments and Mr. SUN Guowu for his help with the original paper.

REFERENCES

Anderson, J. R., and R. D. Rosen, 1983: The latitude-height structure of 40–50-day variations in atmospheric angular momentum. *J. Atmos. Sci.*, **40**(6), 1584–1591.

Barnett, P. T., 1983: Interaction of the monsoon and Pacific trade wind systems at interannual time scales. Part I: The equatorial zone. *Mon. Wea. Rev.*, **111**, 756–773.

Chen Guixing, Li Weibiao, Yuan Zhuojian, et al., 2005: Evolution mechanisms of the intraseasonal oscillation associated with the Yangtze River basin flood in 1998. *Sci. China (Ser. D)*, **48**(7), 957.

Ding Yihui, Li Chongyin, He Jinhai, et al., 2004: South China Sea monsoon experimentation and East Asian summer monsoon. *Acta Meteor. Sinica*, **62**(5), 561–584. (in Chinese)

—— and Ma Xiaoqing, 2008: Analysis of isentropic potential vorticity for a strong cold wave during 2004/2005 winter. *Acta Meteor. Sinica*, **22**(2), 129–141.

Gong Zhensong, Wang Yongguan, and Xu Li, 2004: Middle-high latitude circulation and rainfall of Huaihe River basin in the summer of 2003. *Meteor. Mon.*, **30**(2), 30–33. (in Chinese)

Han Rongqing, Li Weijing, and Dong Min, 2006: The impact of 30–60-day oscillation over the subtropical Pacific on the East Asian summer rainfall. *Acta Meteor. Sinica*, **64**(2), 149–163. (in Chinese)

Hoskins, B. J., M. E. McIntyre, and A. W. Robertson, 1985: On the use and significance of isentropic potential vorticity maps. *Quart. J. Roy. Meteor. Soc.*, **111**(470), 877–946.

Jeong, J. H., B. M. Kim, C. H. Ho, et al., 2008: Systematic variation in wintertime precipitation in East Asia by MJO-induced extratropical vertical motion. *J. Climate*, **21**(4), 788–801.

Jia Yan and Guan Zhaoyong, 2010: Associations of summertime rainfall anomalies over the Changjiang-Huaihe River valley with the interannual variability of 30–60-day oscillation intensity in the western North Pacific. *Chinese J. Atmos. Sci.*, **34**(4), 691–701. (in Chinese)

Ju Jianhua, Qian Chen, and Cao Jie, 2005a: The intraseasonal oscillation of East Asian summer monsoon. *Chinese J. Atmos. Sci.*, **29**(2), 187–194. (in Chinese)

—— and Zhao Erxu, 2005b: Impacts of the low frequency oscillation in East Asian summer monsoon on the drought and flooding in the middle and lower valley of the Yangtze River. *J. Trop. Meteor.*, **21**(2), 163–171. (in Chinese)

——, Sun Dan, and Lu Junmei, 2008: The relay character analysis of the zonal and longitudinal propagations of the atmospheric intraseasonal oscillation in the East Asian monsoon region. *Chinese J. Atmos. Sci.*, **32**(3), 523–529. (in Chinese)

Kalnay, E., M. Kanamitsu, R. Kistler, et al., 1996: The NCEP/NCAR 40-year reanalysis project. *Bull. Amer. Meteor. Soc.*, **77**(3), 437–471.

Lau, K. M., and P. H. Chan, 1985: Aspects of the 40-50-day oscillation during the northern winter as inferred from outgoing longwave radiation. *Mon. Wea. Rev.*, **113**(11), 1889–1909.

Li Chongyin, 1991: Global characteristics of 30-60 day atmospheric oscillation. *Chinese J. Atmos. Sci.*, **15**(3), 66–76. (in Chinese)

—— and Wu Peili, 1990: An observational study of the 30–50-day atmospheric oscillation. Part I: Structure and propagation. *Adv. Atmos. Sci.*, **7**(3), 294–304.

—— and Zhou Yaping, 1994: Relationship between intraseasonal oscillation in the tropical atmosphere and ENSO. *Chinese J. Geophy.*, **37**(1), 17–26. (in Chinese)

Li Huijin, Li Jiangnan, Xiao Hui, et al., 2010: Isentropic potential vorticity analysis on the events of low temperature, freezing rain, and snow in southern China in early 2008. *Plateau Meteor.*, **29**(5), 1196–1207. (in Chinese)

Madden, R. A., and P. R. Julian, 1971: Detection of a 40–50-day oscillation in the zonal wind in the tropical Pacific. *J. Atmos. Sci.*, **28**(5), 702–708.

——, and ——, 1972: Description of global-scale circulation cells in the tropics with a 40–50-day period. *J. Atmos. Sci.*, **29**(6), 1109–1123.

Mao Jiangyu and Wu Guoxiong, 2005: Intraseasonal variability in the Yangtze-Huaihe River rainfall and subtropical high during the 1991 Meiyu period. *Acta Meteor. Sinica*, **63**(5), 762–770. (in Chinese)

Murakami, M., 1979: Large-scale aspects of deep convective activity over the gate area. *Mon. Wea. Rev.*, **107**(8), 994–1013.

North, G. R., T. L. Bell, R. F. Cahalan, et al., 1982: Sampling errors in the estimation of empirical orthogonal functions. *Mon. Wea. Rev.*, **110**(7), 699–706.

Qi Yanjun, Zhang Renhe, Li Tianming, et al., 2008: Impacts of intraseasonal oscillation on the onset and interannual variation of the Indian summer monsoon. *Chinese Sci. Bull.*, **54**(5), 880–884.

Shou Shaowen, 2010: Theory and application of potential vorticity. *Meteor. Mon.*, **36**(3), 9–18. (in Chinese)

Slingo, J. M., K. R. Sperber, J. S. Boyle, et al., 1996: Intraseasonal oscillations in 15 atmospheric general circulation models: Results from an AMIP diagnostic subproject. *Climate Dyn.*, **12**(5), 325–357.

——, D. P. Rowell, K. R. Sperber, et al., 1999: On the predictability of the interannual behavior of the Madden-Julian oscillation and its relationship with El Niño. *Quart. J. Roy. Meteor. Soc.*, **125**(554), 583–609.

Sun Chang, Mao Jiangyu, and Wu Guoxiong, 2009: Influences of intraseasonal oscillation on the clustering of tropical cyclone activities over the western North Pacific during boreal summer. *Chinese J. Atmos. Sci.*, **33**(5), 950–958. (in Chinese)

Sun Guowu, Xin Fei, Chen Bomin, et al., 2008: Apredicting method on the low-frequency synoptic weather map. *Plateau Meteor.*, **27**(Suppl.), 64–68. (in Chinese)

——, Xin Fei, Kong Chunyan, et al., 2010: Atmospheric low-frequency oscillation and extended range forecast. *Plateau Meteor.*, **29**(5), 1142–1147. (in Chinese)

Sun Ying and Ding Yihui, 2008: Effects of intraseasonal oscillation on the anomalous East Asian summer monsoon during 1999. *Adv. Atmos. Sci.*, **25**(2), 279–296.

Tian Hua, Li Chongyin, and Yang Hui, 2010: Modulation of typhoon tracks over the western North Pacific by the intraseasonal oscillation. *Chinese J. Atmos. Sci.*, **34**(3), 559–579. (in Chinese)

Wang Sheng, Tian Hong, Ding Xiaojun, et al., 2009: Climate characteristics of precipitation and phenomenon of drought-flood abrupt alternation during main flood season in Huaihe River basin. *Chinese J. Agrometeor.*, **30**(1), 31–34. (in Chinese)

Wei Fengying, 2007: *Modern Climatic Statistical Diagnosis and Prediction Technology*. China Meteorological Press, Beijing, 63–65. (in Chinese)

Wu Bingyi, Zhang Yan, and Song Yingjie, 1994: The longitudinal propagations and geographical features of the 10–20-day oscillation. *Chinese J. Atmos. Sci.*, **18**(5), 561–568. (in Chinese)

Wu Zhiwei, Li Jianping, He Jinhai, et al., 2006: Large-scale atmospheric singularities and summer long-cycle droughts-floods abrupt alternation in the middle and lower reaches of the Yangtze River. *Chinese Sci. Bull.*, **51**(16), 2027–2034.

Yang Hui and Li Chongyin, 2003: The relation between atmospheric inraseasonal oscillation and the summer severe flood and drought in the Changjiang-Huaihe River basin. *Adv. Atmos. Sci.*, **20**(4), 540–553.

Yang Qiuming, 2001: The drought/flood in the low reaches of Yangtze River and the interannual variations of the 30–60-day oscillation of Eurasian circulation during summer half year. *Acta Meteor. Sinica*, **59**(3), 318–326. (in Chinese)

Yuan Wei and Yang Haijun, 2010: On the modulation of MJO to the precipitation of Southeast China in winter season. *Acta Scientiarum Naturalium Universitatis Pekinensis*, **46**(2), 207–214. (in Chinese)

Zhang, C., 2005: Madden-Julian oscillation. *Rev. Geophys.*, **43**, RG2003, doi: 10.1029/2004RG000158.

Zhang Kesu, 1987: The 40–50-day low-frequency oscillation of the zonal mean flow and its destabilizing effect. *Chinese J. Atmos. Sci.*, **11**(2), 227–236. (in Chinese)

Zhang Lina, Lin Pengfei, Xiong Zhe, et al., 2011: Impact of the Madden-Julian oscillation on pre-flood season precipitation in South China. *Chinese J. Atmos. Sci.*, **35**(3), 560–570. (in Chinese)

Zhang Qin, Ni Yunqi, Lin Wuyin, et al., 1992: Diagnostic study for intraseasonal oscillation of tropical and mid-high latitudes in a low resolution global spectral model. *J. Trop. Meteor.*, **8**(4), 289–296. (in Chinese)

Zhao Liang and Ding Yihui, 2009: Potential vorticity analysis of cold air activities during the East Asian summer monsoon. *Chinese J. Atmos. Sci.*, **33**(2), 359–374. (in Chinese)

Zhu Congwen and Li Jianping, 2004: Modulation of tropical depression cyclone over the Indian-western Pacific Ocean by Madden-Julian oscillation. *Acta Meteor. Sinica*, **62**(1), 42–51. (in Chinese)